Organic Process Research & Development **2009**, *13*, 420–428

Reaction Progress Analysis: Powerful Tool for Understanding Suzuki–Miyaura Reaction and Control of Polychlorobiphenyl Impurity

Sandeep B. Kedia* and Mark B. Mitchell

GlaxoSmithKline Research and Development, Five Moore Drive, Research Triangle Park, North Carolina 27709, U.S.A.

Abstract:

Cross coupling of unsaturated aryl or vinyl triflates/halides with aryl boronic acids using Pd as catalyst (Suzuki coupling) have become increasingly attractive for making the heterocoupled product (Ar–Ar′). However, most Pd cycle reactions produce some homocoupled impurity. This is a major concern when the impurities are polychlorobiphenyls (PCBs). To understand and control the impurity formation was the most important challenge. This contribution demonstrates how reaction progress analysis along with mathematical modeling can be used to gain fundamental understanding and postulate reaction mechanism, providing an insight on how to reduce the amount of byproduct generated in the catalytic cycle with a limited number of experiments (typically three). Fundamentals, such as stability of catalyst, catalyst poisoning, inhibition, and reaction mechanism, can also be answered with these limited number of experiments. Characterization of the catalytic cycle led to a semi-batch addition regime of boronic acid, which effectively eliminated PCB generation by forcing the catalytic cycle to partition between the oxidative addition intermediate (I) and transmetallated intermediate (II).

Introduction

The palladium-mediated cross coupling of aryl or vinyl halides/triflates with aryl boronic acid (Suzuki–Miyaura reaction) has been extensively applied in recent years and is the method of choice for the synthesis of unsymmetrical biaryl systems.[1] Invariably the Suzuki reaction also furnishes low levels of undesired symmetrical biaryls resulting from homocoupling of either the aryl halide[2] or the aryl boronic acid,[3] and while this is generally of little concern, this is not the case when one of the byproducts is a polychlorinated aromatic. The resulting homocoupled biaryls are then, by definition, polychlorinated biphenyls (PCBs) which are strictly controlled in most countries due to both their toxicicity and environmental impact. For example, in the United States most processing plants must control the level of PCBs to <50 ppm, unless the facility is a registered producer of PCBs. For these cases, controlling the impurity formation is a major challenge, requiring a detailed mechanistic understanding of the process.

This contribution describes the utilization of *in situ* collected reaction kinetic profiles in conjunction with appropriate mathematical modeling to gain an understanding of key features of the reaction mechanism. In this example PCB formation stemmed solely from homocoupling of the aryl boronic acid (Scheme 1), and various mechanisms are proposed in the literature for this reaction.[3–5]

Scheme 1. **Suzuki–Miyaura coupling**

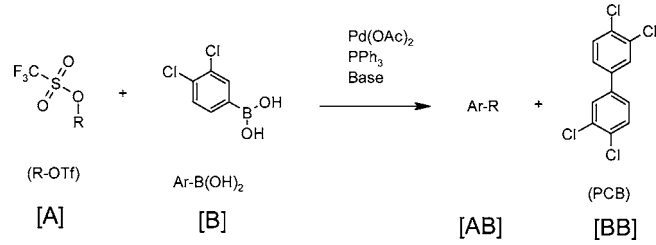

The principles of reaction progress analysis developed by Blackmond[6,7] proved to be invaluable in understanding the catalytic cycle.

Questions To Consider When Performing Pd Cycle Chemistry.

a. Is the catalyst stable?
b. Is the catalyst being poisoned during the course of reaction?
c. Is there substrate/product inhibition observed by catalyst?
d. At what stage in the catalytic cycle is the impurity formed?
e. Does the kinetic profile fit the mechanism; do we understand the mechanism?

We demonstrate here that by following the methodology described by Blackmond, one can answer those questions in a limited number of experiments (typically less than 5).

Reaction

A catalyst–base–solvent screen had identified the optimal reagents to effect the Suzuki–Miyaura coupling of vinyl triflate [A] with aryl boronic acid [B] (Scheme 1) while minimizing the level of the undesired PCB.[8] However, despite this the amount of PCB generated was still 2–5% compared to product. This limited the manufacturing of the current product to less than 5 kg of product/year in order to comply with the state environmental regulations. The main goal of the kinetic study was to understand the characteristics of the *normal* reaction, since knowledge of the desired catalytic cycle and resting states

* Author to whom correspondence may be sent. E-mail: sandeep.b.kedia@gsk.com.

(1) (a) Miyaura, N.; Suzuki, A. *Chem. Rev.* **1995**, *95*, 2457. (b) Bellina, F.; Carpita, A.; Rossi, R. *Synthesis* **2004**, 2419.
(2) Tsou, T.; Kochi, J. *J. Am. Chem. Soc.* **1979**, *103*, 7547.
(3) Moreno-Manas, M.; Perez, M.; Pleixats, R. *J. Org. Chem.* **1996**, *61*, 2346.
(4) Adamo, C.; Amatore, C.; Ciofini, I.; Jutand, A.; Lakmini, H. *J. Am. Chem. Soc.* **1979**, *103*, 7547.
(5) Smith, G.; Dezeny, G. *J. Org. Chem.* **1994**, *59*, 8151.
(6) Blackmond, D. *Angew. Chem., Int. Ed.* **2005**, *44*, 4302.
(7) Blackmond, D. *J. Org. Chem.* **2006**, *71*, 4711.
(8) Deschamps, N.; Elitzin, V.; Tabet, E. GSK unpublished data.

Published on Web 01/20/2009

10.1021/op800205x CCC: $40.75

of intermediate species is central to understanding where impurity generation occurs, and hence its subsequent control.

Rate Expression for Suzuki−Miyaura Coupling. Literature precedent[1] indicates a catalytic cycle with two intermediate species is most likely for the Suzuki−Miyaura reaction, as depicted in Scheme 2. The right-hand cycle depicts the proposed

Scheme 2. **Postulated mechanism for the catalytic cycle for desired product formation (Ar-R)**

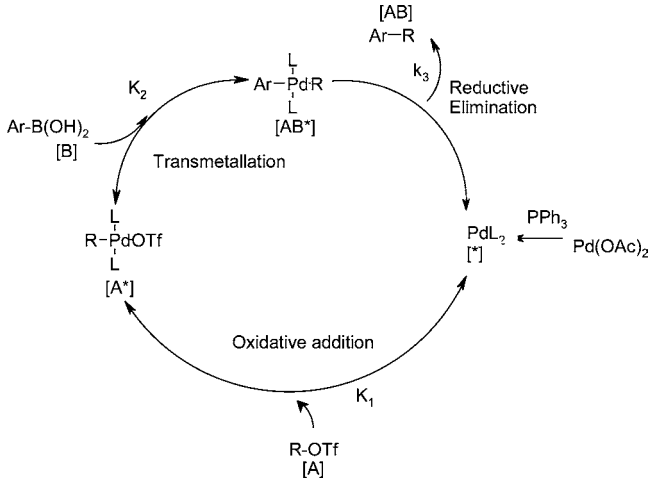

competing catalytic process for PCB generation.[3] The rate equation for a two-intermediate catalytic process can be derived[9] as follows from consideration of the fundamental reaction steps:

1. Activation of Pd-sites with triphenyl phosphine ligand [L], assumed to be very fast reaction:

$$[\mathrm{Pd}(0)] + 2[\mathrm{L}] \rightarrow [*]$$

2. Oxidative addition of Ar-triflate [A] with active Pd*:

$$[*] + [\mathrm{A}] \underset{k_{-1}}{\overset{k_1}{\rightleftharpoons}} [\mathrm{A}^*]$$

3. Transmetalation; insertion of boronic acid into Pd-catalyst:

$$[\mathrm{A}^*] + [\mathrm{B}] \underset{k_{-2}}{\overset{k2}{\rightleftharpoons}} [\mathrm{AB}^*]$$

4. Reductive elimination; product formation and regeneration of active Pd-catalyst:

$$[\mathrm{AB}^*] \xrightarrow{k_3} [\mathrm{AB}] + [*]$$

The rate of formation of the desired product is given by:

$$\mathrm{rate}[\mathrm{AB}] = k_3[\mathrm{AB}^*] \quad (1)$$

The quasi-equilibrium assumption is used to derive an expression for the concentration of the bound species:

$$[\mathrm{AB}^*] = K_2[\mathrm{A}^*][\mathrm{B}] \quad (2)$$

$$[\mathrm{A}^*] = K_1[\mathrm{A}][*]_{Active} \quad (3)$$

Substitution of eqs 2 and 3 into the initial rate expression (eq 1) gives the following rate equation:

$$\mathrm{rate}[\mathrm{AB}] = K_1K_2k_3[\mathrm{A}][\mathrm{B}][*]_{\mathrm{Active}} \quad (4)$$

From mole balance for catalyst (Pd):

$$[*]_{\mathrm{Total}} = [*]_{\mathrm{Active}} + [\mathrm{A}^*] + [\mathrm{AB}^*] \quad (5)$$

Substitution of eqs 2 and 3 into eq 5 and rearrangement yields:

$$[*]_{\mathrm{Active}} = \frac{[*]_{\mathrm{Total}}}{1 + K_1[\mathrm{A}] + K_1K_2[\mathrm{A}][\mathrm{B}]} \quad (6)$$

Substituting eq 6 into eq 4 gives the desired overall rate expression for the catalytic cycle as:

$$\mathrm{rate}[\mathrm{AB}] = \frac{K_1K_2k_3[\mathrm{A}][\mathrm{B}][*]_{\mathrm{Total}}}{1 + K_1[\mathrm{A}] + K_1K_2[\mathrm{A}][\mathrm{B}]} \quad (7)$$

where $K_i = k_i/k_{-i}$

Experimental Procedures

In the current example, all kinetic studies were performed using an iChemExplorer[10] equipped for heating and stirring. Use of iChemExplorer allowed reactions to be performed directly in the HPLC vial, with the convenience of rapid direct injection HPLC sampling and automated profile generation. Thus, by using a small quantity of substrate (~100 mg), one can perform profiling very rapidly, thereby gaining insight into the reaction mechanism.

In a 2-mL HPLC vial, 1 mL of toluene was added along with vinyl triflate (1 equiv), boronic acid (1 equiv + excess defined in Table 1), Hunig's base (1.6 equiv), water (15 equiv), triphenyl phosphine (0.3 or 0.6 equiv, see Table 1) and palladium acetate (0.1 or 0.2 equiv, see Table 1). A magnetic stirrer was inserted, and the vial was crimped to minimize solvent loss from sampling. The vial was then inserted into the iChemExplorer block which was then heated to 70 °C and stirred. Samples were collected at 3-min intervals. The overall

Table 1. **Same excess and different excess experiments**

exp	boronic acid (mol/L)	triflate (mol/L)	$Pd(OAc)_2$ (mol/L)	excess (mol/L)
1	0.059	0.030	0.006	0.030
2	0.059	0.030	0.003	0.030
3	0.052	0.022	0.003	0.030
4	0.118	0.030	0.003	0.089
5	0.047	0.018	0.006	0.030
6	0.044	0.030	0.006	0.015

(9) Rawlings, J.; Ekerdt, J. *Chemical Reactor Analysis and Design Fundamentals*; Nob Hill Publishing Co.: Madison, WI, 2002.

(10) *IChemExplorer*; Reaction Analytics Inc.: Wilmington, DE, 2008; http://www.ichemexplorer.com.

rate is calculated from first principles using eq 7 (refer to Determining the Rate-Limiting Step section below for details).

The initial goal of the experiments was to confirm a first-order dependence upon catalyst (eq 7) and to explore if the catalyst activity was affected by reaction progression, allowing us to rule in or out complicating factors such as substrate inhibition, product inhibition, and reaction induction. Once demonstrated, a handle on the catalytic cycle and specifically the resting states of the catalytic species could then be determined. Overall, six experiments were conducted (Table 1), comprising some at varying catalyst load (to probe order in catalyst), some at the *same reagent excess* (to probe catalyst activity), and some at *different reagent excess* (to probe the catalytic cycle).

Two sets of experiments (10 mol % and 20 mol %) were run to identify if there was any saturation of Pd sites with R-OTf during the onset of these reactions and identify the resting state in each set of experiments. The calculated concentration of vinyl triflate was within 5% of measured value at 95% confidence level.

Normalizing the Reaction Rate: Use of the Excess Concept. *Excess* [e] is the difference in molar concentration between the two substrates for a bimolecular reaction. The *excess* for a given experiment is constant, and does not change as the reaction progresses.

$$[e] = [B]_i - [A]_i = [B]_f - [A]_f \Rightarrow [B]_t = [e] + [A]_t \quad (8)$$

[A] = vinyl triflate; [B] = boronic acid; excess = [e] = [B] − [A];
i = initial condition, f = final condition;
t = at time point t

Use of the catalytic rate expression (eq 7) to describe the kinetics for a given reaction assumes that catalyst activity is not affected by variation in reagent concentrations. In practice it is not uncommon for the catalyst to be activated or deactivated by components in the reaction mixture, e.g. substrate inhibition, product inhibition, poisoning, and catalyst induction. The first goal of the kinetic analysis is to determine if such issues are at play, and this is achieved by comparing two or more *same excess* experiments with differing starting substrate concentrations.

If the reaction rate is now plotted against substrate concentration (either boronic acid or vinyl triflate) for two *same excess* experiments differing only in initial substrate concentrations, then the plots should exactly overlay if catalyst activity is invariant between the reactions. This has been done for experiments 1 and 5 (Figure 1), the exact overlay showing that catalyst activity is indeed identical for the two experiments.

Accordingly, the total concentration of active catalyst sites is the same in both cases and is unaffected by the catalyst history. For instance, as experiment 1 proceeds, the reactant concentrations will eventually wane to the initial concentrations for experiment 5. The graphical overlay plot indicates that the catalyst activity for the two reactions remains the same (as expected from eq 7) even though for the case of reaction 1 the catalyst has performed many turnovers and is now in the presence of a significant concentration of product. Similarly, when we normalize the rate by dividing by catalyst concentration (since [catalyst] varied across the experiments) and plot it versus [A], we now see overlay for all of the *same excess* experiments 1, 2, 3, and 5 (Figure 2).

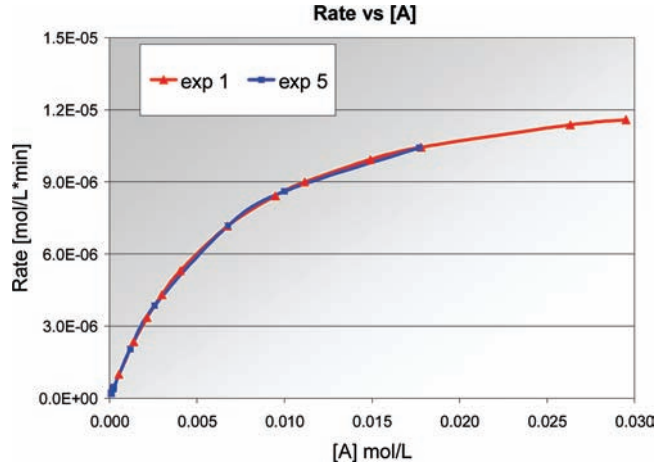

Figure 1. **Rate vs concentration of vinyl triflate for *same excess* experiments 1 and 5.**

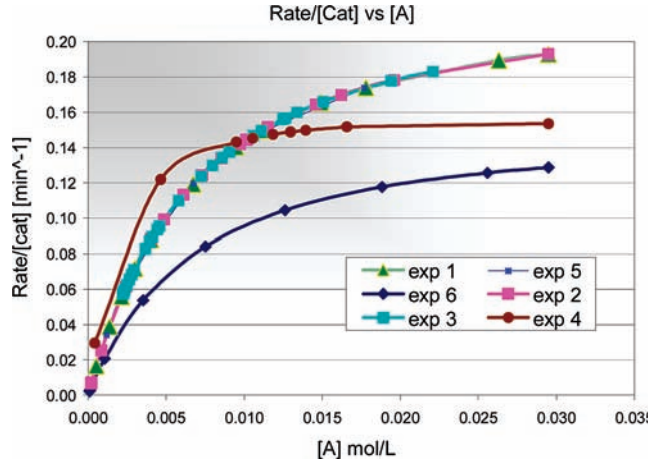

Figure 2. **Normalized rate {rate/[cat]} versus vinyl triflate for all six experiments.**

In both cases (Figure 1 and Figure 2) we see that different excess experiments 4 and 6 do not overlay; we will discuss more about this in graphical methodology below.

Determining the Rate-Limiting Step. Blackmond has applied spreadsheet calculators[11] to understand the kinetics of the catalytic cycle through derivation of the underlying reaction constants. To determine the rate-limiting step in our reaction, rate and equilibrium constants in eq 7 were required, and this seemed the most logical approach to obtain these values. We accordingly applied this approach, utilizing a spreadsheet modified from a version supplied to us by Blackmond.[11]

Measurements can be either *differential data* which is directly related to the reaction rate (e.g., calorimetric power) or *integral data* which is directly related to concentration (e.g., IR or UV absorption). In our case we

(11) GSK in-house training course: Blackmond, D. *Kinetics of Organic Catalytic Reactions*; GSK Chemical Development: Philadelphia, PA, U.S.A., 2007.

have *integral data* since we are measuring the area under curve of an HPLC UV response, and since we know the initial concentration of reactants and that reaction proceeds to completion (with only low levels of byproduct formation) it is both simple and valid to simply scale the UV response to concentration units for the reactant we are tracking the disappearance of. Accordingly, the normalized concentration of one of the substrates $[A]_{measured}$, i.e., R-OTf is measured with respect to time using this approach. From this, the concentration of [B] is determined at each time point from the known excess in the experiment = [A] + [e]. Using these concentrations, the rate of reaction is calculated at each point by using eq 7 (initially choosing some arbitrary values for constants K_1, K_2, and k_3). The rate of reaction for consecutive data points ($r_{AB,1}$ at t_1 and $r_{AB,2}$ at t_2) is calculated using eq 7, then $[A]_{calc}$ is derived at t_2 by eq 9, which is simply the concentration at t_1 minus the product of the sampling interval and the average rate over the sampling interval. This works well for a high sampling frequency (as employed in these experiments) and clearly $[A]_{calc}$ at t_0 is set to the known initial concentration of A.

$$[A]_{calc,2} = [A]_{calc,1} - (r_{AB,1} + r_{AB,2}) * (t_2 - t_1)/2 \quad (9)$$

The goal is to minimize the error between $[A]_{measured}$ and $[A]_{calc}$ (using the least mean square (LMS) method) and to fit simultaneously the same rate and equilibrium constants (K_1, K_2 and k_3) across all six experiments (same and different excess and differing catalyst loading). For our reactions the values obtained for the constants are listed in Table 2.

Table 2. **Calculated rate and equilibrium constants**

rate constants		units	errors (10^{-2})
K_1	5.24	L/mol	±1.04
K_2	979.	L/mol	±20.3
k_3	0.22	min^{-1}	±0.34

See Figure 3 for measured versus predicted concentration of [A]. Once the three reaction constants (K_1, K_2, k_3) have been synchronously fitted across all six experiments (using LMS regression), then one can confidently use eq 7 to calculate the rate of reaction under any of the experimental conditions. It should be noted that the biggest source of pure error is in the measurement of the reactant concentration, with some discontinuities evident in Figure 3 clearly stemming from this. It should be remembered, however, that the reaction constants are synchronously fitted across all the experiments, which has the effect of minimizing the overall pure error in the calculated reaction constants (since the residuals should, on average, sum close to zero over multiple measurements). All plots related to rate should accordingly be smooth (as seen); however, the fitted concentration profile in Figure 3 mirrors the discontinuities arising from experimental error in the measurements. Although this may look surprising, it is quite expected when you remember that $[A]_{calc}$ is determined at each point using the mean calculated rate between that point and the immediately preceding point (eq 9). This is in turn evaluated with eq 7 and the *measured* values of [A] at the consecutive points. Hence, the calculated concentrations at these points will be skewed by the pure error in the measured values, resulting in the calculated concentrations mirroring the error in the measurements. This is of little consequence since it is the rate and equilibrium constant information that is of prime importance, and as described earlier, the synchronous fitting tends to minimize the overall error in these values.

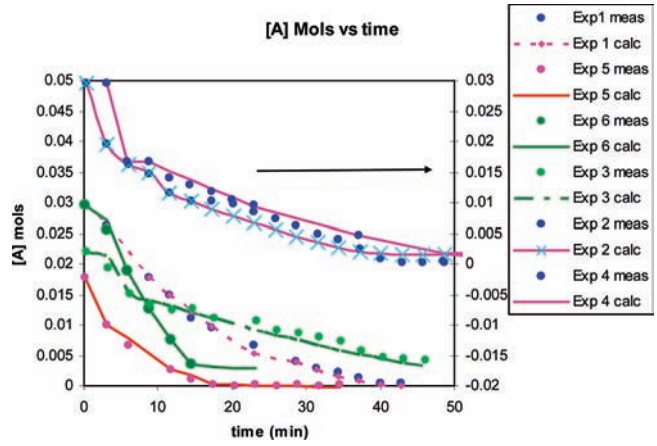

Figure 3. **Finding rate constants using LMS method by minimizing error between measured concentration and calculated concentration of [A] using eqs 7 and 9 simultaneously.**

To shed some more light on the resting state of the catalyst and intermediate species, graphical methodology was used in conjunction with the above data.

The difference between the calculated concentration of vinyl triflate and the measured value was within ±5% at 95% confidence level. The mean difference was 1.3% with standard deviation of 1.9%.

Introducing the Graphical Rate Equation. Inspection of eq 7 suggests there may be some merit in plotting the rate of reaction divided by concentration of one of the reactants against the concentration of the other reactant. This is an example of a *graphical rate equation*, and looking for the overlay of plots for experiments of known excess is central to the kinetic analysis methodology.[6] We will later apply this equation for reactions with *different excess*; however, it is also instructive to apply it now for the *same excess* experiments (1, 2, 3, and 5). In Figure 4, the rate of reaction divided by the concentration of boronic

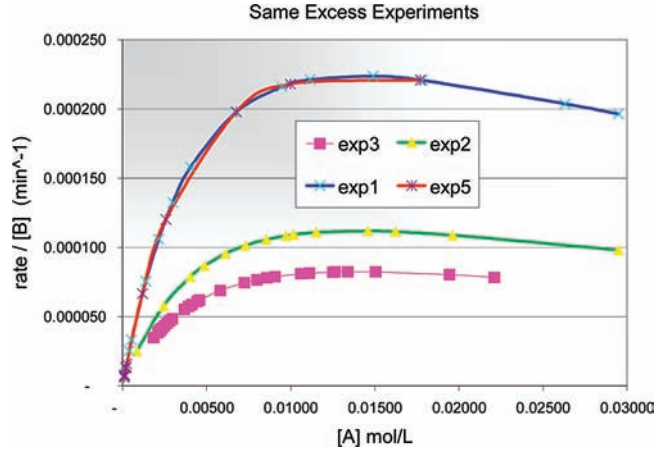

Figure 4. **Graphical rate equation for same excess experiments.**

acid ([B]) is plotted against the concentration of vinyl triflate ([A]), where it can be seen that the plots for experiments 1 and 5 exactly overlay, while those for experiments 2 and 3 do not.

Note, however, that the catalyst concentration for experiments 2 and 3 differs from that for experiments 1 and 5. Recall that one of the initial objectives was to prove the first-order dependence upon catalyst given in eq 7, and we have not yet accounted for this in the *graphical rate equation* depicted in Figure 4. Instead, if we plot the rate of reaction divided by the product of boronic acid concentration ([B]) and total catalyst concentration ([C]), we should obtain an exact overlay of all the curves if the catalyst dependence is first order. This is depicted in Figure 5, where the first-order dependence on catalyst is clearly demonstrated by the exact overlay of the plots.

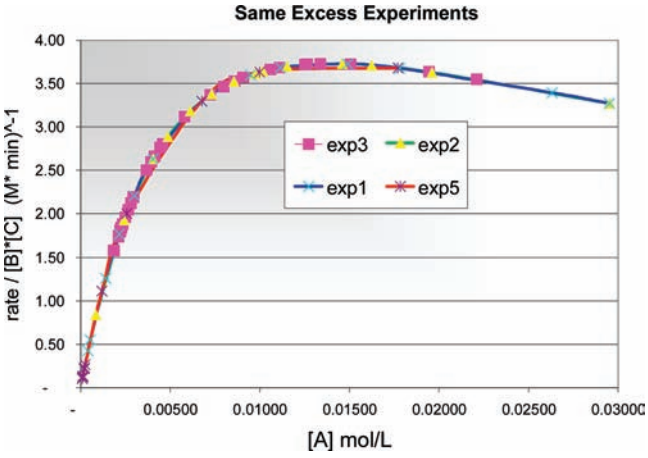

Figure 5. **First-order dependence in catalyst is demonstrated.**

It could also be concluded a first-order dependence on [B] based upon the overlap of these plots; however, there is an issue here. We somewhat arbitrarily chose to plot rate/[B] vs [A], and from eq 8 we know [B] and [A] are related by the reagent *excess*. Because of this relationship, if we had plotted Rate/[A] vs [B] it would have also directly overlaid; by considering only *same excess* experiments we cannot distinguish between these scenarios—this is somewhat akin to trying to solve simultaneous equations in three unknowns with only two equations. To solve the problem we need a third equation, and that equation is a *different excess* experiment.

Probing the Catalytic Cycle: the Different Excess Experiment. From the overlay of the *same excess* experiments we can confidently conclude that the catalyst is robust with the kinetics following the expected rate equation (eq 7). We have also seen that there is a first-order dependence upon [A] or [B] but that we cannot distinguish between these cases. In Figure 6 the rate of reaction divided by the product of [B] and [C] is plotted against [A] for the *same excess* experiments (as *per* Figure 5) and also for the *different excess* experiments (experiments 4 and 6).

The exact overlay of the plots immediately tells us the reaction is first order in [B] {at low [A]} and [C] since the rate was normalized by the product of [B] and [C]. Recall we had already proved the first-order dependence on [C] from the *same excess* experiments; the additional overlay with a different *excess experiment* provides additional confirmation. Also at low

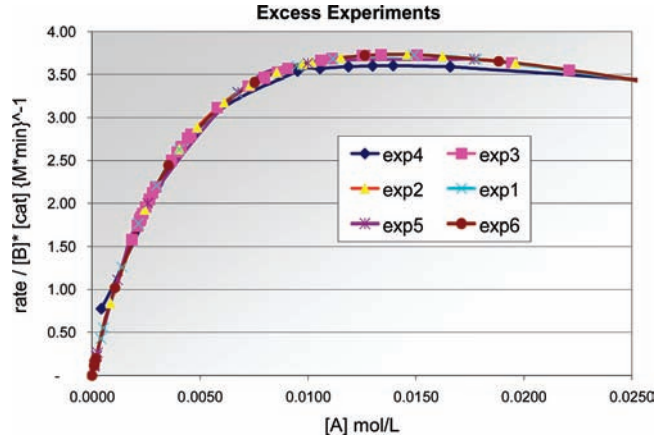

Figure 6. **First-order dependence upon [A] and [B] demonstrated at low [A] concentration.**

[A], it can be seen that the rate doubles with doubling the [A], indicative of first order in [A] at concentrations below 0.005 M.

A Closer Look at the Graphical Rate Equation (for high [A] concentration). We have so far demonstrated a robust catalyst system with a first-order dependence upon aryl boronic acid and vinyl triflate at low [A] concentration, but what is the dependence on [A] above 0.005 M? To answer this question we need to plot the rate of reaction divided by [C] against [A] or [B] {see Figure 7}.

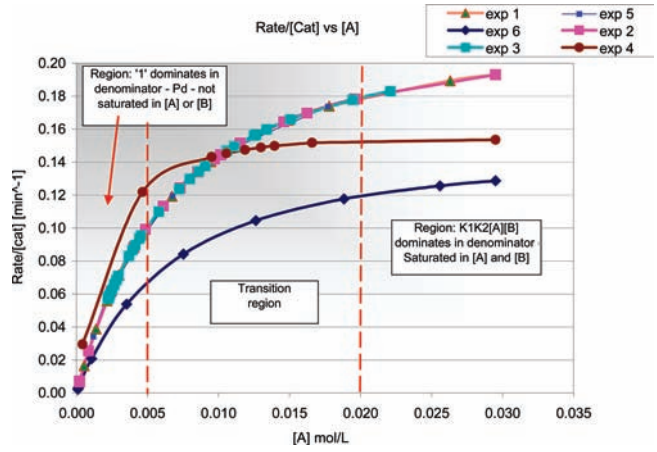

Figure 7. **Normalized rate/[C] vs [A].**

From Figure 7, it can be seen that for high[12] [A] (greater than 0.02 M), rate divided by [C] is nearly constant, indicative of zero order in both [A]- and [B]-saturated regions. Whereas,

(12) At high [A], the [B] is necessarily high since it is in excess.

(13) For LC−MS analysis, the catalyst was forced to sit entirely at (I) by omitting aryl boronic acid from the reaction mixture (as described in the text). HPLC analysis shows complete conversion to (I) which when analyzed by ESI LC−MS furnished a peak with MW = 884, corresponding to $[M-OTf]^+$ for the complex $RPd(PPh_3)_2OTf$. The MS also displayed the characteristic isotopomer pattern for a Pd complex. The characterization of an analogous complex by ESI LC−MS during Pd-catalyzed reductive carbonylation has recently been reported, the intermediate also ionizing as [M−X] in this instance (ref 16). Such complexes clearly have significant aqueous stability and survive ESI LC−MS conditions. This is perhaps unsurprising, since for the case of Suzuki reaction, water often accelerates the reaction (as is the case for our reaction), and use of water as the primary solvent is often employed in the literature for this type of coupling (ref 17).

at low [A] {concentration less than 0.005 M}, the normalized rate doubles with doubling the concentration of [A] or [B], indicative of first order in [A] and [B] for low [A], under-saturated. The region between 0.005 and 0.02 M is where the mechanism transitions from the resting state of the catalyst being at [II] to being partitioned between [I] and [III], see Figures 8 and 9. Although not illustrated, the same conclusion can be drawn for B when plotting rate/[C] vs [B].

This is a demonstration of *saturation kinetics*, at high [A] and [B] the catalyst is fully saturated in both A and B and the reaction rate is constant—zero order in [A] and [B]. At low [A] and [B] the reaction is second order overall—first order in both [A] and [B]. The implications for the catalytic cycle are depicted in Figures 8 and 9.

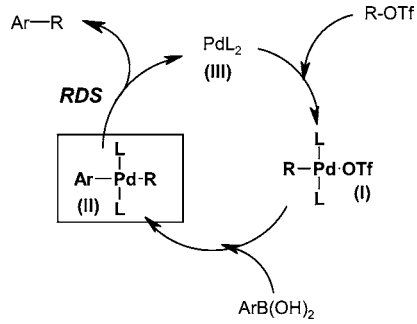

Figure 8. **Catalytic cycle for saturation kinetics. Catalyst fully saturated in vinyl triflate and aryl boronic acid, resting state is (II), and rate-determining step is reductive elimination step.**

$$rate[AB]=K_1K_2k_3[A][B][*]_{Total}$$

("1" term dominates denominator in Eqn.(7))

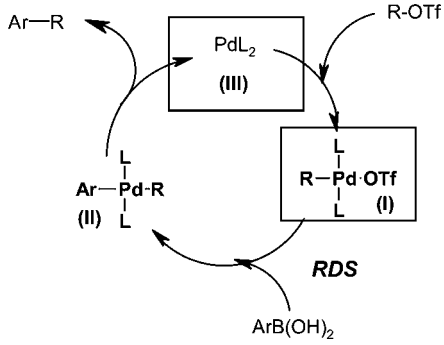

Figure 9. **Catalytic cycle during the end of reaction. Catalyst is not saturated, resting states are partitioned between (III) and (I). Rate-determining step is addition of the boronic acid.**

The above could have also been obtained by using the rate constants. It could be easily be shown that the product of K_1K_2[A][B] $\gg 1 + K_1$[A] in the denominator of eq 7, for concentration greater than 0.02 M of [A]. Also the term '1' dominates ($1 \gg K_1$[A] $+ K_1K_2$[A][B]) in the denominator for concentration of [A] less than 0.005 M, hence showing how the rate-determining step shifts during the catalytic cycle.

Impurity Reduction/Elimination. Kinetic analysis of the *normal reaction* allows us to delineate the resting states of the "on-cycle" intermediates; under saturation kinetics the transmetallated intermediate (II) is the resting state (Figure 8), while under unsaturated conditions the catalyst rests at both the Pd(0)L_2 stage (III) and at (I). This is crucial information for understanding control of homocoupling, since we can now postulate the mechanism for formation of PCB where the intermediate (III) is common to both the *normal reaction* and *impurity generation* in the catalytic cycles (see Scheme 3). In this report no attempt has been made to investigate the kinetics of PCB formation as this is out of the scope of this work. Here we demonstrate that, with the kinetic profile for the main reaction and knowing the various resting states, one can easily delineate the plausible mechanism for PCB formation and avoid the catalyst resting at (III) to minimize the impurity.

At the start of the reaction the concentrations of vinyl triflate and aryl boronic acid are high, and the reaction proceeds under saturation kinetics, the resting state of the catalytic cycle sitting at (II). As the concentrations of reactants fall, the catalyst becomes under-saturated, and the catalytic cycle now partitions between both intermediates (I) and (III), providing an opportunity for effective competing homocoupling of aryl boronic acid to occur. This arises since a tangible concentration of intermediate (III) now exists in solution to undergo the much slower oxidative addition with the aryl boronic acid. In contrast, when the catalyst was saturated with reactants, intermediate (III) did not reach any significant concentration since it is consumed as fast as it is formed by rapid oxidative addition into the vinyl triflate.

The increasing rate of formation of symmetrical biaryl PCB can be seen in Figure 10 (blue curve) for batch Suzuki—Miyaura coupling in direct response to an increasing partition towards (III) as the reaction progresses. Interestingly, real-time HPLC profiling was able to track an intermediate species which was confirmed as the oxidative addition intermediate (I) by LC—MS.[13] As the reaction approaches completion, this intermediate rapidly disappears, commensurate with consumption of all the vinyl triflate.

To minimize PCB formation we clearly need to force the catalytic cycle to rest at either (I) or (II) for the duration of the whole reaction. At low [B] we know that transmetalation with aryl boronic acid is rate limiting, so by removing aryl boronic acid from the reaction mixture completely, we can force the catalytic cycle to sit at intermediate (I), that is [I] = $[*]_{Total}$, all added palladium exists as (I). *Addition of aryl boronic acid is this manner is atypical for Suzuki—Miyaura-type reactions, as almost all reactions are done in batch fashion for these types of cross-coupling reactions.* Aryl boronic acid should now be added semi-batch in a "feed controlled" manner; that is to say as aryl boronic acid is added, it is immediately consumed and does not accumulate in solution to any appreciable level. This is synonymous with a rate of addition slower than the instantaneous rate of vinyl triflate oxidative addition. If true, this will force the catalytic cycle to partition between (I) and (II), and we will have effectively slowed down the transmetalation step by limiting the reagent concentration.

Scheme 3. **Postulated mechanism for catalytic cycle for desired product formation on the left (Ar-R), and the impurity (PCB) on the right**

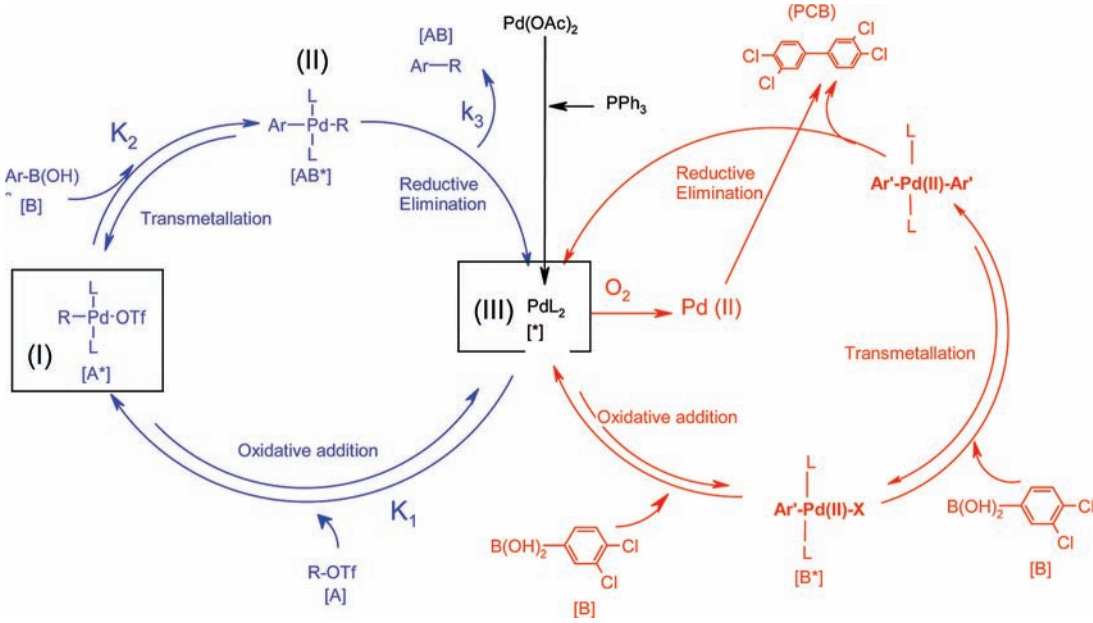

PCB Control by Semi-Batch Addition. Accordingly, control of PCB formation was demonstrated through semi-batch addition of aryl boronic acid, which was added as a solution to the reaction mixture over 3−6 h. Various temperatures were explored (60, 70, 80, and 90 °C), under which the reaction went to completion in all cases without significant PCB formation. Reaction profiles for the semi-batch additions under the various temperatures can be seen in Figures 11−14, each resulting in negligible PCB formation.

Some literature reports[4] suggest oxidation of Pd(0) to Pd(II) is required for homocoupling of the aryl boronic acid. However, we were confident from our kinetic analysis that the catalyst would be partitioning between the oxidative addition intermediate (I) and transmetallated intermediate (II), and this implied that oxygen should have minimal effect upon the reaction. Comparing the two reactions side by side, one performed open to air, the other employing rigorous degassing and nitrogen purging, indeed furnished comparable results. Both afforded product with <50 ppm PCB content (Figure 15).

A reaction temperature of 70 °C was chosen for subsequent scale-up at 1 L whence product was obtained as expected, again with negligible PCB formation (<10 ppm).

For semi-batch addition of aryl boronic acid, no aryl boronic acid was detected by real time HPLC profiling, confirming "feed controlled" addition rate slower than the overall reaction rate. HPLC also detected two intermediates, the red line corresponding to the oxidative addition intermediate (I) confirmed by LC−MS. The second intermediate (blue line) was of fleeting existence and could

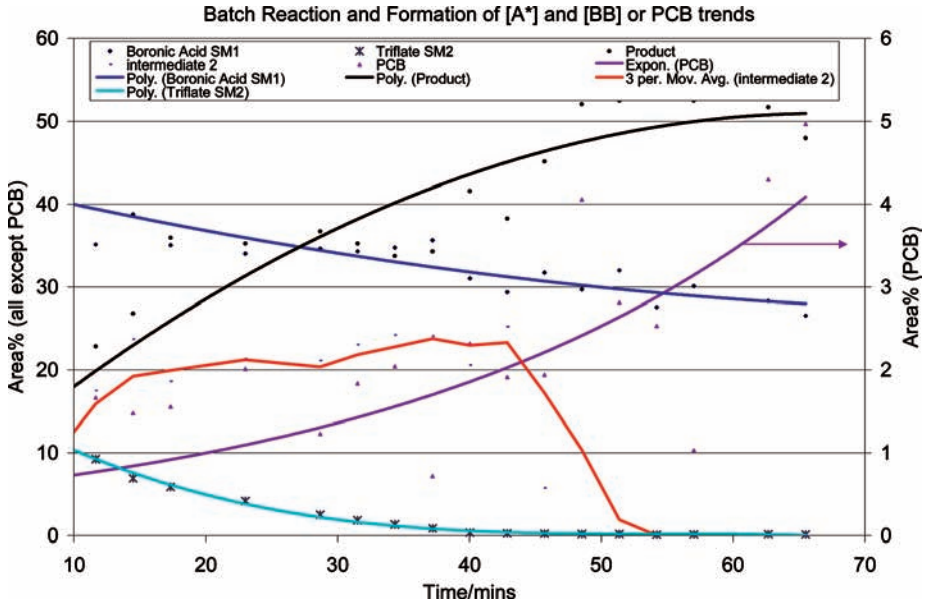

Figure 10. **Batch Suzuki coupling in the presence of excess aryl boronic acid.**

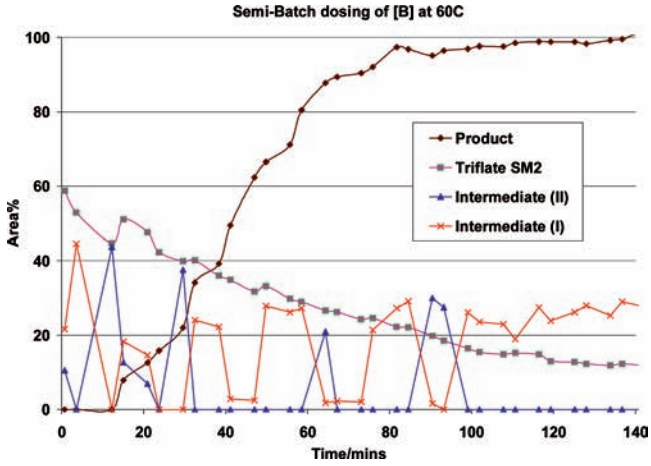

Figure 11. **Semi-batch addition of boronic acid at 60 °C.**

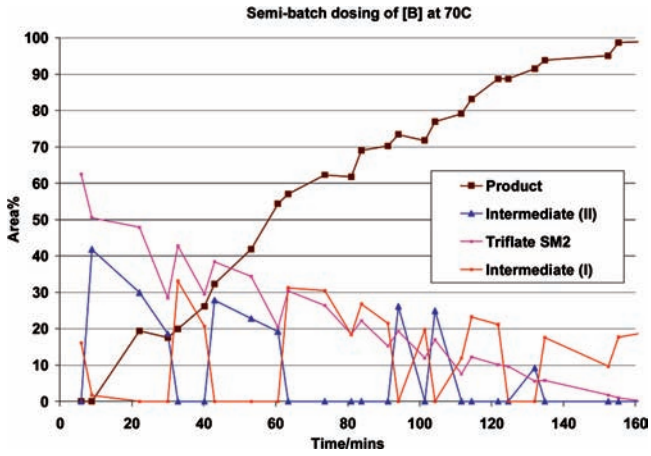

Figure 12. **Aryl boronic acid addition at 70 °C.**

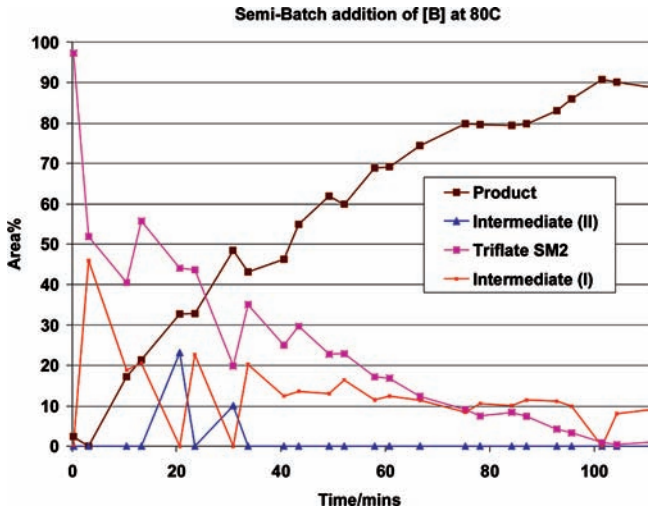

Figure 13. **Aryl boronic acid addition at 80 °C.**

not be confirmed by off-line LC−MS, but it is postulated this is the transmetallated intermediate (II). This is consistent with feed-controlled enforced partition between (I) and (II), and depending upon when the HPLC pulls a sample for direct inject, one or other of these intermediates may be predominating. As the reaction proceed, the RDS will naturally shift towards transmetalation (as in the batch reaction) so we would expect to mostly observe intermediate (I) in the latter stages of the addition which is what

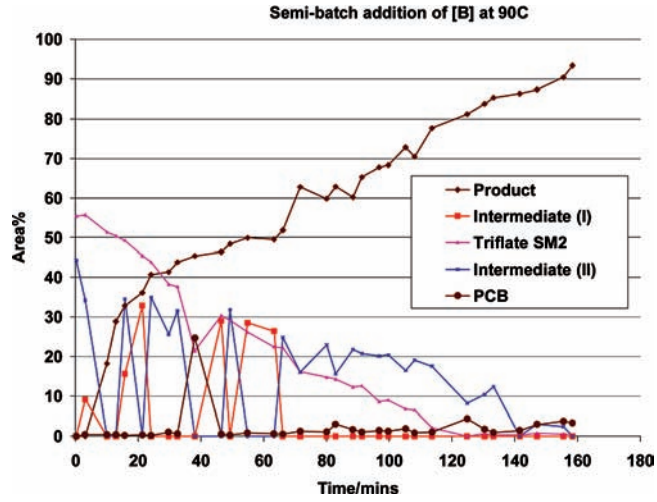

Figure 14. **Aryl boronic acid addition at 90 °C.**

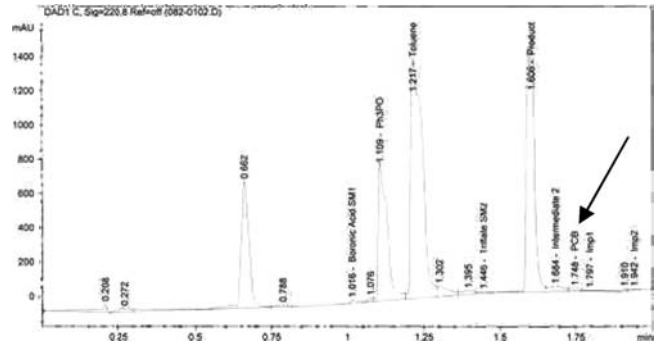

Figure 15. **HPLC profile for scale-up run on a 1-L scale.**

was observed. No PCB was seen by HPLC (level of detection is ∼100 ppm). This behavior appears to be borne out experimentally for all the cases studied (Figures 11, 12, 13, and 14).

PCB level was found to be 7.4 ppm in reaction solution. PCB concentration (shown above with arrow) in not detected on HPLC column, for a concentrated reaction mixture, indicating <100 ppm PCB present in reaction mix (LOD ≥ 100 ppm).

Conclusions

Reaction profile analysis and application of the graphical rate equation has facilitated control of PCB generation through understanding of the catalytic cycle. Specifically we have:

i demonstrated the catalyst is stable and rugged from the *same excess* experiments;
ii demonstrated the dependence upon aryl boronic acid and vinyl triflate from the *different excess* experiments;
iii demonstrated catalyst sits at transmetallated intermediate {(II)} at high concentrations of reactants (saturation kinetics) and rests between oxidation addition intermediate {(I)} and active Pd(0) {(III)} otherwise;
iv delineated cycle must rest at oxidation additive intermediate {(I)} or transmetallated intermediate {(II)} to minimize PCB formation;
v employed semi-batch addition of aryl boronic acid to enforce partition between oxidation additive and transmetallated intermediates {(I) and (II), respectively};

vi successfully reduced PCB levels to <50 ppm;
vii demonstrated that oxygen sensitivity[14,15] was not the cause of PCB formation in this example.

Acknowledgment

We thank the project leader, Matthew J. Sharp; process chemists, Vassil Elitzin, Elie Tabet, and Nicole Deschamps, for their valuable contributions that aided in understanding this catalytic system, for their postulation of the mechanism, along with their support in the kinetics work. We also thank Robert Yule for his support to the kinetics team; John Grimes, David Black, and Kim Harvey for their valuable support in identifying the intermediate structures and for analytical support throughout the course of this work.

Note Added after ASAP: The errors in Table 1 have been corrected for the version published on the Internet April 7, 2009.

(14) Coifini, I. *J. Am. Chem. Soc.* **2006**, *128*, 6829.
(15) Smith, M. *Adv. Synth. Catal.* **2005**, *347*, 647.
(16) Beller, M. *J. Am. Chem. Soc.* **2008**, *130*, 15549.
(17) See for example: Moore, L.; Shaughnessy, K. *Org. Lett.* **2004**, *6*, 225.

Received for review August 22, 2008.

OP800205X